Metal-Insulator Transition Induced by Short Range Magnetic Ordering in Mono-layered Manganite

E. O. Chi, W. S. Kim, C. S. Hong, N. H. Hur,* and Y. N. Choi†

Center for CMR Materials, Korea Research Institute of Standards and Science, Yusong, P.O. Box 102, Daejeon 305-600, Korea
†Neutron Physics Department, HANARO center, Korea Atomic Energy Research Institute, Yusong, P.O. Box 105, Daejeon 305-600, Korea
Received December 17, 2002

The structural, magnetic, and transport properties of a mono-layered manganite $La_{0.7}Sr_{1.3}MnO_{4+\delta}$ were investigated using variable temperature neutron powder diffraction as well as magnetization and transport measurements. The compound adopts the tetragonal *I4/mmm* symmetry and exhibits no magnetic reflection in the temperature region of 10 K ≤ T ≤ 300 K. A weak ferromagnetic (FM) transition occurs about 130 K, which almost coincides with the onset of a metal-insulator (M-I) transition. Extra oxygen that occupies the interstitial site between the [(La,Sr)O] layers makes the spacing between the [MnO_2] layers shorten, which enhances the inter-layer coupling and eventually leads to the M-I transition. We also found negative magneto resistance (MR) below the M-I transition temperature, which can be understood on the basis of the percolative transport *via* FM metallic domains in the antiferromagnetic (AFM) insulating matrix.

Key Words : Magnetism, Manganese oxide, Magnetic ordering

Introduction

The observation of colossal magnetoresistance (CMR) in perovskite manganite $Ln_{1-x}A_xMnO_3$ (*Ln* = lanthanide; *A* = Ca, Sr) that considers as the $n = \infty$ member of the Ruddlesden-Popper series $(Ln,A)_{n+1}Mn_nO_{3n+1}$ has stimulated to investigate other numbers of this family.[1] In particular, the $n = 2$ phase $La_{2-2x}Sr_{1+2x}Mn_2O_7$ has been extensively studied due to its unique anisotropy and dimensionality effects.[2-4] The bi-layered manganite behaves in a similar manner as found in the three-dimensional perovskite manganite. Although its Curie temperature (T_C) is reduced due to reduction of 3*d*-band width, it shows a M-I transition accompanied by the onset of ferromagnetism and exhibits large negative MR near T_C.[5]

In contrast to what occurs for the bi-layered manganite, the M-I transition typically concomitant with T_C has not been observed yet in the $n = 1$ homologue, which consists of [MnO_2] layers separated along the *c*-axis by a rock-salt type [$(La,Sr)_2O_2$] layer (see Figure 2). Instead, the mono-layered compound exhibits an insulating property combined with the AFM or spin-glass-like state.[6,7] Recently, Moritomo *et al.* identified the absence of both metallic nature and FM ordering from the studies on single crystals of $La_{1-x}Sr_{1+x}MnO_4$ ($0.0 \le x \le 0.7$).[8] Interestingly, they observed the disappearance of the AFM transition and the subsequent development of the spin-glass phase for $x \ge 0.2$ at low temperature, which is due to the competing interaction between the AFM superexchange and the FM double exchange. More recently, Maignan *et al.* studied the $Ca_{2-x}Ln_xMnO_4$ ($0.0 < x \le 0.2$; *Ln* = Pr, Sm, Gd, Ho) compound with an orthorhombic symmetry and reported that negative MR is present in the insulating Ca-substituted manganite with high doping concentration.[9]

Thus far, the mono-layered manganites have been explored mainly with the expectation that they will render new insights and interesting physical properties compared with other members of the Ruddlesden-Popper series. Finding of the M-I transition associated with the CMR property in the mono-layered system would thus be interesting to understand the interplay between the change in dimensionality and the resulting physical phenomenon, which eventually helps to elucidate the underlying mechanism of the manganite physics. From our comprehensive studies on polycrystalline sample of $La_{0.7}Sr_{1.3}MnO_{4+\delta}$, we are able to claim that a M-I transition and negative MR below the M-I transition temperature indeed exist in the mono-layered manganite system although they are not accompanied by the long-range FM ordering but induced by short-range type magnetic ordering. In addition, a plausible mechanism on the M-I transition and negative MR found in $La_{0.7}Sr_{1.3}MnO_{4+\delta}$ is discussed on the basis of percolative transport *via* FM metallic domain in the AFM insulating matrix as proposed by Uehera *et al.*[10]

Experimental Section

Precursor material with nominal composition of $La_{0.7}Sr_{1.3}MnO_4$ was prepared from stoichiometric amounts of $SrCO_3$, dry La_2O_3, and Mn_2O_3 by the conventional solid state reaction route. In the course of synthesizing the layered manganite, we found that the perovskite phase is grown solely on the surface of the pellet.[11] To prevent the formation of the perovskite impurity, we have thus employed new encapsulation method in which a calcined pellet of $La_{0.7}Sr_{1.3}$-

*To whom correspondence should be addressed. E-mail: nhhur @kriss.re.kr

MnO_4 is completely covered with the same calcined powder. The encapsulated pellet was then sintered at 1,560 °C in air for 30 h two times. The purity of the samples was carefully examined by powder X-ray diffraction. This technique, which prevents the pellet from contacting with air and crucible, turns out to be very advantageous to prepare perovskite-free sample of $La_{0.7}Sr_{1.3}MnO_{4+\delta}$ (within X-ray and neutron resolution limit). In order to ensure the reproducibility on the synthesis of $La_{0.7}Sr_{1.3}MnO_{4+\delta}$ as well as its structural, magnetic and transport data, sample preparation and measurement were repeated several times under the same conditions. Neutron powder diffraction data for structural refinement were collected as a function of temperature on a high-resolution powder diffractometer at HANARO Center in KAERI. The 2θ range is from 0° to 160° with a step size of 0.05°. A neutron source with λ = 1.8346 Å supplied by Ge (331) single crystal monochromator was used. The neutron diffraction data were analyzed with the Rietveld technique using the Fullprof program,[12] revealing that the compound adopts tetragonal *I4/mmm* symmetry in the whole measured temperature range from 10 to 300 K.

Results and Discussion

The lattice parameters and the Mn-O bond lengths as a function of temperature are plotted in Figure 1(a) and 1(b), respectively. The experimental data for the lattice changes are well fitted by second order polynomial equation of temperature shown in dashed lines. Indeed, the *c*-lattice parameters are in excellent agreement with the calculated values obtained from one polynomial equation. The axial Mn-O1 bond length *d*(Mn-O1), given in Figure 1(b), have large standard deviations owing to degree of freedom of the O1 atomic position. Accordingly, a fitting with any polynomial equation is meaningless. On the other hand, the *a*-lattice data are fitted well with two equations, which shows a deviating behavior near 150 K. As anticipated from the temperature evolution of the lattice parameters, the equatorial Mn-O2 bond length *d*(Mn-O2) (see Figure 2), is also fitted with two polynomial equations and an anomalous deviation is observed near 150 K. The deviating temperature is almost coincident with the onset of the weak FM ordering as discussed below (Figure 3(a)). This is certainly attributed to the magnetoelastic effect, where the magnetic exchange interaction of the Mn spins within the [MnO_2] layer leads to shrinkage of the equatorial Mn-O2 bond length in the *ab*-plane. This unique structural variation near 150 K implicates that a close correlation between lattice and spin exists in this system. Similar phenomenon was also found not only in other members of Ruddlesden-Popper series such as n = 2

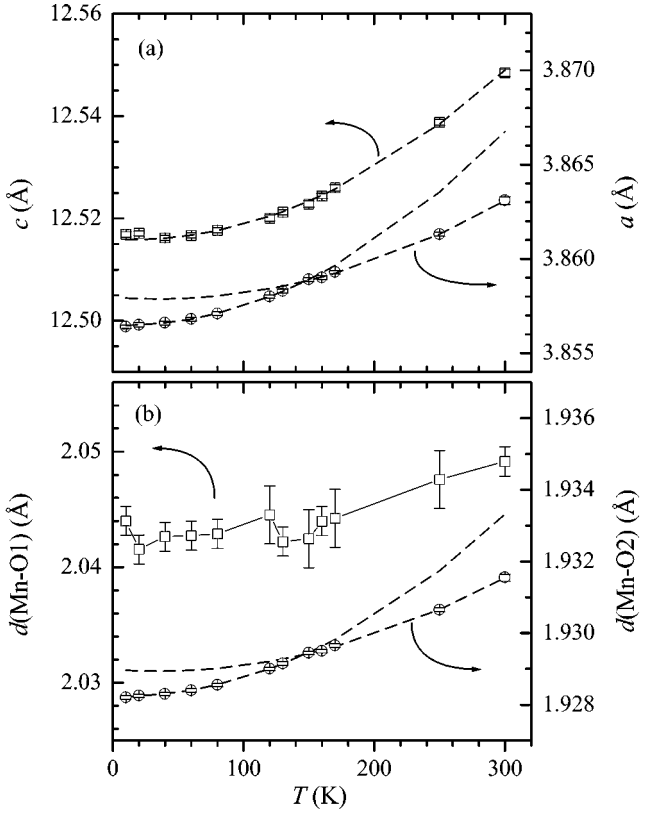

Figure 1. (a) Temperature dependence of lattice parameters of *a* (open circle) and *c* (open rectangular) and (b) Variations of the Mn-O1 (open rectangular) and Mn-O2 (open circle) bond lengths for $La_{0.7}Sr_{1.3}MnO_{4+\delta}$. Dashed lines are fitting curves.

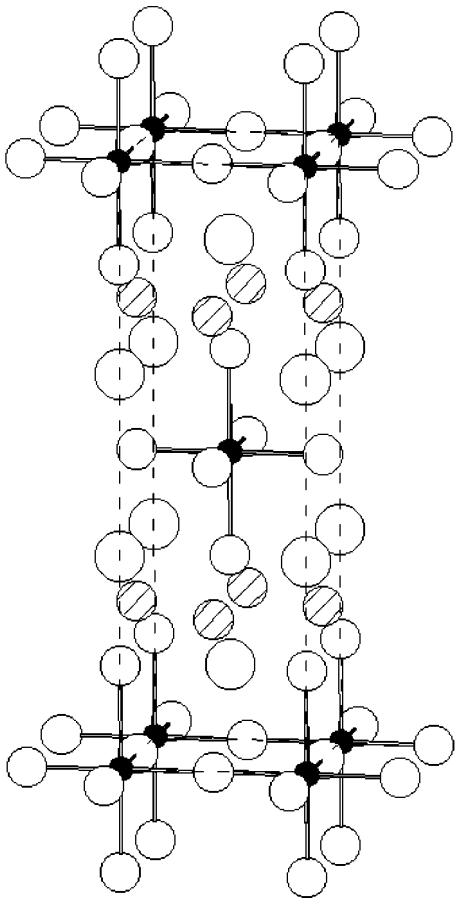

Figure 2. Structure of $La_{0.7}Sr_{1.3}MnO_{4+\delta}$. Large open circles, small open circles and hatched circles represent La/Sr atoms, oxygen atoms and interstitial oxygen O3 atoms, respectively.

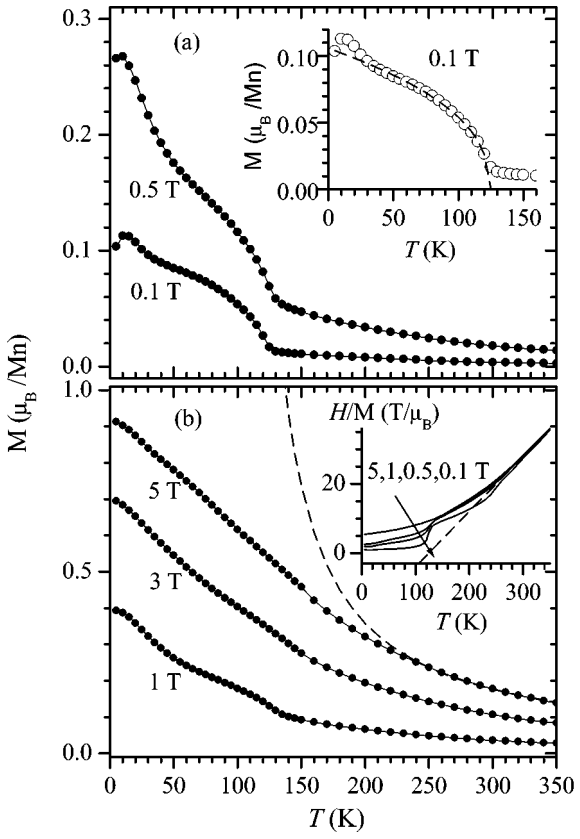

Figure 3. (a) Temperature dependent magnetization data of $La_{0.7}Sr_{1.3}MnO_{4+\delta}$ obtained at applied fields of 0.1 T and 0.5 T. The inset shows a fitting curve (dashed line) with a power law of $M(T) = M_0(1–T/T^*)^{\beta}$. (b) Temperature dependent magnetization data at higher applied fields of 1, 3 and 5 T (solid circle) and a Curie-Weiss fitting curve (dashed line). The inset shows the inverse magnetization *H*/M curves and a Curie-Weiss fitting curve (dashed line).

and $n = \infty$ but also in an antiperovskite $GaCMn_3$ compound.[13-15]

It is worthy to recall that the magnetic interaction between the $[MnO_2]$-layers separated by the intervened insulating $[(La,Sr)_2O_2]$-layers, namely along the *c*-axis, is considerably weak mainly due to weak magnetic moment. In the bi-layered manganites, however, a significantly larger response of the *c*-axis on the FM ordering is found,[16] implying that the magnetic ordering in $La_{0.7}Sr_{1.3}MnO_{4+\delta}$ takes place as a short-range type. This conjecture is supported by the results of the Rietveld refinements on the neutron diffraction data in that any magnetic Bragg peaks were not observed down to 10 K. An important feature in the structure of $La_{0.7}Sr_{1.3}MnO_{4+\delta}$, given in Figure 2, is that additional oxygen O3 located at the interstitial site between the two [(La/Sr)O] layers is present. Although only 1.5% of the oxygen position determined by both idometric titration and neutron diffraction is occupied, the interstitial oxygen results in a contraction along the *c* axis as found in the oxidized phase of $La_{1.2}Sr_{0.8}MnO_{4+\delta}$.[17] Particularly, the Mn-Mn distance between the $[MnO_2]$ layers, 6.274 Å, is substantially reduced compared to that of a single crystal of $La_{0.7}Sr_{1.3}MnO_4$ (6.300 Å).[18] Interestingly, the inter-layer distance of the present polycrystalline compound is in between the single crystal of $La_{0.7}Sr_{1.3}MnO_4$ and the bi-layered mangnite $La_{1.4}Sr_{1.6}Mn_2O_7$ (6.235 Å). It is worthy to mention that the latter compound shows metallic and long-range ordered FM behavior.[16] The shrinkage of the inter-layer distance induced by the interstitial oxygen appears to play an important role in controlling the magnetic and transport properties of $La_{0.7}Sr_{1.3}MnO_{4+\delta}$ that will be discussed.

Temperature dependent magnetization curves of $La_{0.7}Sr_{1.3}MnO_{4+\delta}$ obtained at applied fields of 0.1 T and 0.5 T are shown in Figure 3(a). The M(*T*) curve at 0.1 T displays an ordinary FM signature in the temperatures ranging from 135 K to about 30 K although it is not a long-range ordered transition. The dashed line in the inset of Figure 3(a) is the power-law fit with the expression of $M(T) = M_0(1–T/T_C)^{\beta}$. Interestingly, the β value, which is 0.407, is rather close to the three dimensional (3D) Heisenberg one (0.365), implying that the magnetic transition has a 3D character and also the inter-layer magnetic interaction is feasible. As can be seen in the fitting curve, there is a slight deviation below 30 K, which is ascribed to the competing interaction between the AFM and FM phases. This is in good agreement with the spin-glass transition as observed in magnetization data of a single crystal. It is important to mention that the M(*T*) curves of the single crystal does not show any weak FM transition except for the Curie-Weiss-like behavior in the high temperature regime.[8] This discrepancy in the magnetization data is presumably ascribed to the interstitial oxygen that will be discussed.

Another notable feature in the M(*T*) data is that total magnetic moment shown in Figure 3(b) is enhanced with increasing a magnetic field. As a result, the FM phase is suppressed by the field and eventually smeared out at 5 T. Moreover, the M(*T*) curves are deviated from the Curie-Weiss-like behavior, which are calculated from the Curie-Weiss fitting to the magnetization data in high temperature range of 250 K-350 K (dashed line in Figure 3(b)). As given in the inverse susceptibility *H*/M curves shown in the inset of Figure 3(b), all the curves begin to deviate from the Curie-Weiss curves near 250 K and lie below the fitting line. This is a clear evidence for the existence of the AFM component. However, any indication of the AFM ordering such as a drop in the magnetization or a cusp-like behavior has not been found in the M(*T*) curves because the AFM ordering is a short-range ordered type. This is fully consistent with the results of neutron diffraction refinements, where any magnetic peaks were not detected in all measured temperature range from 10 to 300 K.

Taken together, our results clearly reveal that both the FM and AFM orderings exist as a short-range type. Indeed, the FM moment obtained from extrapolating the fitting curve to 0 K is found to be only about 0.1 μ_B/Mn at 0.1 T, which is shown in the inset of Figure 3(a). Moreover, the magnitude of the FM moment is scarcely influenced by the higher applied field. The field induced magnetic moment reaches to about 0.85 μ_B/Mn at 5 K and 5 T, which is much larger than the FM one. It is thus conceivable that the induced-moment is originated from the AFM phase, which is dominant

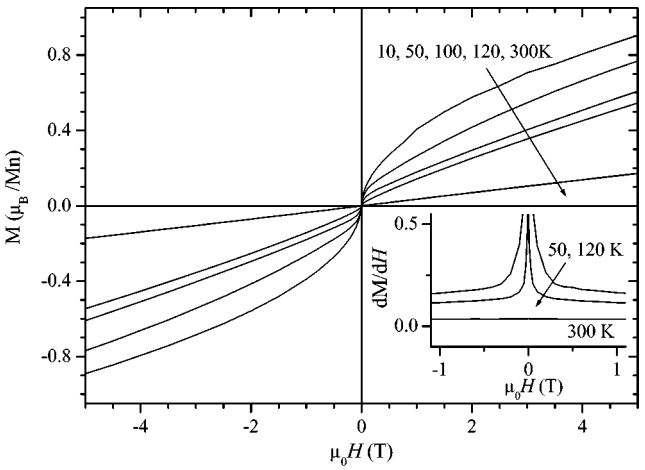

Figure 4. Magnetization (*M*) versus magnetic field (*H*) curves for $La_{0.7}Sr_{1.3}MnO_{4+\delta}$ at various temperatures. The inset shows d*M*/d*H* curves.

particularly in the high magnetic field. It is worthy to note that we have recently revealed the existence of long-range FM ordering even in the mono-layered manganite $La_{0.5}Sr_{1.5}Mn_{1-x}Ru_xO_4$, in which the Ru doping creates ferromagnetism.[19]

The coexistence of the two different short-range ordered phases is also evidenced by the magnetization hysteresis curves, which are displayed in Figure 4. The M(*H*) curves of $La_{0.7}Sr_{1.3}MnO_{4+\delta}$ above 120 K are almost linear in *H*, indicating a paramagnetic state. The constant value of d*M*/d*H* given in the inset of Figure 4 also implicates the presence of the paramagnetic phase. Below 120 K, however, two different slopes are clearly shown in the d*M*/d*H* curves. One slope in the low field range, $|\mu_0H| < 0.5$ T, is certainly ascribed to the FM component. The other one with a nearly constant d*M*/d*H* value in the high field region, $|\mu_0H| > 0.5$ T, is caused by the field-induced AFM moment. Consequently, the temperature and field dependent magnetization curves provide clear evidences to show that in $La_{0.7}Sr_{1.3}MnO_{4+\delta}$ short-range FM phase exists in the short-range AFM matrix. It is thus reasonable to consider that the magnetic and transport properties of $La_{0.7}Sr_{1.3}MnO_{4+\delta}$ are largely governed by the competing interaction between the two phases.

Figure 5(a) displays the temperature dependence of resistivity $\rho(T)$ for $La_{0.7}Sr_{1.3}MnO_{4+\delta}$ measured at various magnetic fields. An M-I transition clearly appears near $T_{MI} \approx 160$ K and negative MR occurs below this temperature. Remarkably, T_{MI} is almost close to the onset of the weak FM transition, implying that this concomitant behavior is somewhat relevant to the origin of CMR observed in the perovskite and bi-layered manganites.[1,2] Upon application of magnetic field, T_{MI} very slightly shifts toward higher temperature ($\Delta T_{MI} < 10$ K at $\Delta\mu_0H = 5$T) with respect to that of the typical double exchange type FM manganite in which T_{MI} systematically moves to higher temperature due to suppression of spin fluctuation.[20] Such a tiny shift of T_{MI} in $La_{0.7}Sr_{1.3}MnO_{4+\delta}$ is ascribed to small fraction of the short-range ordered FM phase. This implies that the double

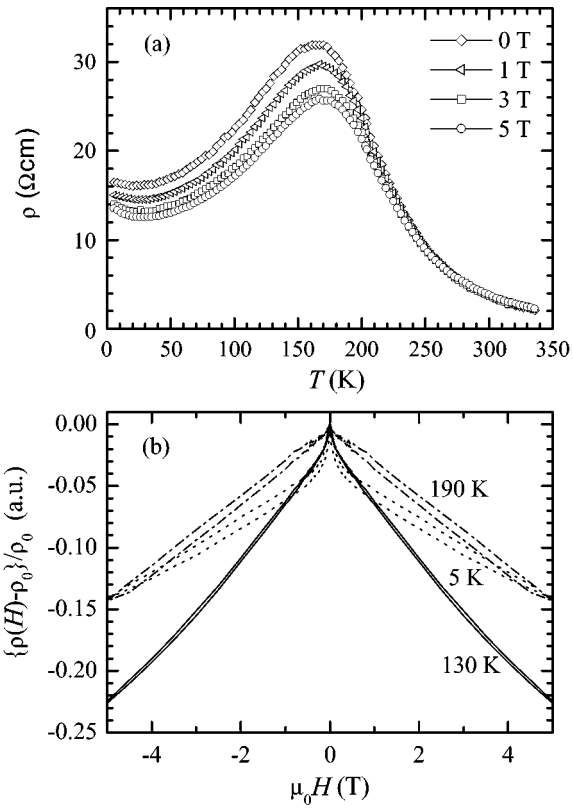

Figure 5. (a) Temperature dependence of resistivity for $La_{0.7}Sr_{1.3}MnO_{4+\delta}$ under different applied magnetic fields. (b) Isothermal magnetoresistance curves of $La_{0.7}Sr_{1.3}MnO_{4+\delta}$ at various temperatures.

exchange mechanism is still operative even in the short-range ordered FM state. The drop of the $\rho(T)$ curves below T_{MI}, taken at various fields, appears to show the temperature independent MR behavior, which is largely due to the field induced alignment of antiferromagnetically coupled Mn spins originated from the AFM phase. Similar behavior in the $\rho(T)$ curves has been observed in the bi-layered manganites with magnetic rare earth elements $Ln_{1.4}Sr_{1.6}Mn_2O_7$ (*Ln* = Pr, Nd, Sm).[21-23]

In order to elucidate the nature of the transport property of $La_{0.7}Sr_{1.3}MnO_{4+\delta}$ further, we have investigated the isothermal MR at various temperatures as a function of applied fields. As shown in Figure 5(b), the shape of the MR curves defined as $\{\rho_H - \rho_0\}/\rho_0$ is slightly different from below and above $T_{MI} \approx 160$ K. The MR decreases almost linearly with *H* at 190 K but exponentially at 5 K as reported in other CMR materials.[24] It should be mentioned that the occurrence of a hysteretic behavior in the paramagnetic state is unusual, where the MR typically varies with H^2.[24] This is a strong evidence for the existence of non-paramagnetic state above T_{MI}. This hysteretic behavior found in both temperature ranges above and below T_{MI} is mainly attributed to the field-induced alignment of antiferromagnetically coupled magnetic moments. On the other hand, a steep increase of MR in the low-field range of $|\mu_0H| < 0.5$ T below T_{MI} is associated with the FM phase, which is consistent with the magnetization data in the inset of Figure 4. This also hints at the existence

of two spatially different phases, namely, the FM metallic and AFM insulating states. Because the AFM component is dominant compared to the FM phase, the MR value of $La_{0.7}Sr_{1.3}MnO_{4+\delta}$ induced by the applied field is just about 22% at 130 K (doted line) even at 5 T. Much higher applied field is required to saturate the AFM spins as shown in Figure 3(b) and 4. Combined with the magnetic and transport results discussed above, we thus conjecture that the M-I transition and the negative MR can be understood on the basis of the percolative transport *via* short-range ordered FM metallic domains in the AFM insulating matrix as suggested by Uehara *et al.*[10]

Among the results discussed above, one of the most critical issues to be discussed is whether the magnetic and transport properties obtained from $La_{0.7}Sr_{1.3}MnO_{4+\delta}$ are intrinsic. Based on the following three reasons, we are able to claim that all the observed data stem from the mono-layered manganite rather than the plausible perovskite impurity. First, a slope change in the temperature dependent variation of the equatorial Mn-O2 bond length that occurs near the weak FM ordering temperature can not be driven by small impurity phases even if they are included in our sample. As a result, the magnetostrictive effect is indeed originated from the $La_{0.7}Sr_{1.3}MnO_{4+\delta}$ compound.[25] It is worthy to remark that a magnetic signal due to negligible amount of perovskite phase included in the bi-layered manganite, which is not detected by X-ray diffraction, is clearly resolved using a SQUID magnetometer.[24] However, we have not seen any other magnetic signals in the entire temperature range besides the weak FM transition near 130 K. Second, the perovskite phase $La_{1-x}Sr_xMnO_3$ that considers as the most likely impurity shows the onset of FM ordering typically in the higher temperature range above 200 K.[24] Finally, the M-I transition cannot be induced by the impurity or inter-grown phases alone because a minimal volume fraction to connect percolation path is at least about 20%.[26]

Another important feature to be addressed is that neither weak FM ordering nor M-I transition has been observed in single crystal of the mono-layered manganite. This remarkable discrepancy might be due to the interstitial oxygen only present in the polycrystalline sample. The extra oxygen, which is located in between the [(La,Sr)O] layers, leads to shorten the *c*-lattice parameter. In particular, the inter-layer distance between the [MnO_2] layers of polycrystalline sample is significantly shorter than that of single crystal.[8,18] These differences are certainly due to the extra interstitial oxygen (δ = 0.060) present in the polycrystalline sample. The interstitial oxygen is typically found in other mono-layered metal oxides such as $Sr_2RuO_{4+\delta}$, $La_2NiO_{4+\delta}$, and $La_2CuO_{4+\delta}$.[27-29] An interesting common feature is that the physical properties of all these materials are very sensitive to the content of extra oxygen.

We now turn to discuss how the interstitial oxygen influences on the physical property. It is worthy to recall that the inter-layer spacing of polycrystalline sample lies in a midway between those of the bi-layered manganite $La_{1.4}Sr_{1.6}Mn_2O_7$ with a metallic and FM character and the single crystal of the mono-layered manganite that has an insulating and AFM property. This clearly implicates that the inter-layer coupling between the [MnO_2] layers plays an important role in determining the physical property. In the layered manganite system, the double exchange interaction in the Mn-O-Mn network is easy to operate in the [MnO_2] plane rather than along the *c*-axis direction due to the intervened [$(La,Sr)_2O_2$] layers that disrupt the interaction between the [MnO_2] layers. When the interstitial site is occupied by oxygen as shown in Figure 2, however, the extra oxygen makes the *c*-axis shorten, which leads to enhance the inter-layer coupling and eventually results in the enlargement of the one-electron 3*d*-band width. This conjecture is in principle fully analogous to the pressure effect as observed in the bi-layered manginites, where the application of pressures reduces the inter-layer distance and induces a M-I transition accompanied by a FM ordering.[30,31] Within this context, the increase in bandwidth of the polycrystalline $La_{0.7}Sr_{1.3}MnO_{4+\delta}$ compound induced by the interstitial oxygen leads to stabilize the FM interaction and enhance the itinerancy of the charge carriers. Therefore, a weak FM ordering and a M-I transition is not unrealistic in the mono-layered manganite system if the interstitial site is optimally doped by oxygen.

Conclusion

We have found that a M-I transition accompanied by short-range FM ordering indeed exists in the mono-layered manganite $La_{0.7}Sr_{1.3}MnO_{4+\delta}$. An important feature is that the weak FM ordering is also closely correlated with the lattice contraction induced by the interstitial oxygen. Moreover, the magnetic and transport properties of the mono-layered manganite are strongly dependent upon the extra oxygen. Negative MR observed below the weak FM transition temperature can be understood by the percolative transport through the short-range FM metallic domains in the AFM insulating matrix. Our magnetic and transport results observed in the $La_{0.7}Sr_{1.3}MnO_{4+\delta}$ compound will thus provide new perspective to understand the layered manganite with the low-dimensional structure.

Acknowledgement. We would like to thank D. Y. Kim at Seoul National University for various helpful conversations. The Creative Research Initiative Program supported this work.

References

1. Jin, S.; Tiefel, T. H.; McCormack, M.; Fastnacht, R. A.; Ramesh, R.; Chen, L. H. *Science* **1994**, *264*, 413.
2. Kimura, T.; Tokura, Y. *Annu. Rev. Mater. Sci.* **2000**, *30*, 451.
3. Battle, P. D.; Green, M. A.; Laskey, N. S.; Millburn, J. E.; Radaelli, P. G.; Rosseinsky, M. J.; Sullivan, S. P.; Vente, J. F. *Phys. Rev. B* **1996**, *54*, 15967.
4. Mitchell, J. F.; Argyriou, D. N.; Jorgensen, J. D.; Hinks, D. G.; Potter, C. D.; Bader, S. D. *Phys. Rev. B* **1997**, *55*, 63.
5. Moritomo, Y.; Asamitsu, A.; Kuwahara, H.; Tokura, Y. *Nature*

1996, *380*, 141.
6. Bao, W.; Chen, C. H.; Carter, S. A.; Cheong, S.-W. *Solid State Commun*. **1996**, *98*, 55.
7. Sternlieb, B. J.; Hill, J. P.; Wildgruber, U. C.; Luke, G. M.; Nachumi, B.; Moritomo, Y.; Tokura, Y. *Phys. Rev. Lett*. **1996**, *76*, 2169.
8. Moritomo, Y.; Tomioka, T.; Asamitsu, A.; Tokura, Y. *Phys. Rev. B* **1995**, *51*, 3297.
9. Maignan, A.; Martin, C.; Van Tendelo, G.; Hervieu, M.; Raveau, B. *J. Mater. Chem*. **1998**, *8*, 2411.
10. Uehara, M.; Mori, S.; Chen, C. H.; Cheong, S.-W. *Nature* **1999**, *399*, 560.
11. Dho, J.; Kim, W. S.; Choi, H. S.; Chi, E. O.; Hur, N. H. *Solid State Commun*. **2001**, *117*, 517.
12. Roisnel, T.; Rodriguez-Carvajal, J. *Program: Fullprof*; LLB-LCSIM: France, March, 2000.
13. Argyriou, D. N.; Mitchel, J. F.; Potter, C. D.; Bader, S. D.; Kleb, R.; Jorgensen, J. D. *Phys. Rev. B* **1997**, *55*, R11965.
14. Ibarra, M. R.; Algarabel, P. A.; Marquina, C.; Blasco, J.; Garcia, J. *Phys. Rev. Lett*. **1995**, *75*, 3541.
15. Kim, W. S.; Chi, E. O.; Kim, J. C.; Choi, H. S.; Hur, N. H. *Solid State Commun*. **2001**, *119*, 507.
16. Chi, E. O.; Hong, K. P.; Kwon, Y.-U.; Raju, N. P.; Greedan, J. E.; Lee, J. S.; Hur, N. H. *Phys. Rev. B* **1999**, *60*, 12867.
17. Li, R. K.; Greaves, C. *J. Solid State Chem*. **2000**, *153*, 34.
18. Hong, C. S.; Kim, W. S.; Chi, E. O.; Hur, N. H.; Choi, Y. N. *Chem. Mater*. **2002**, *14*, 1832.
19. Hong, C. S.; Kim, W. S.; Hur, N. H.; Choi, Y. N. *J. Am. Chem. Soc.*, submitted.
20. De Gennes, P. G. *Phys. Rev.* **1960**, *118*, 141.
21. Hur, N. H.; Kim, J.-T.; Yoo, K. H.; Park, Y. K.; Park, J. C.; Chi, E. O.; Kwon, Y.-U. *Phys. Rev. B* **1998**, *57*, 10740.
22. Kim, W. S.; Chi, E. O.; Choi, H. S.; Yi, H. S.; Hur, N. H.; Kim, J.-T.; Kim, Y. I.; Lee, K. W.; Park, Y. K. *J. Korean Phys. Soc*. **2001**, *38*, 29.
23. Hur, N. H.; Chi, E. O.; Kwon, Y.-U.; Yu, J.; Kim, J.-T.; Park, Y. K.; Park, J. C. *Solid State Commun*. **1999**, *112*, 61.
24. Kim, W. S.; Choi, H. S.; Nam, B. C.; Chi, E. O.; Hur, N. H. *Phys. Status Solidi: Condensed Matter* **2001**, *185*, 401 and references therein.
25. Bader, S. D.; Osgood III, R. M.; Miller, D. J.; Mitchel, J. F.; Jiang, J. S. *J. Appl. Phys.* **1998**, *83*, 6385.
26. Kim, K. H.; Uehara, M.; Hess, C.; Sharma, P. A.; Cheong, S.-W. *Phys. Rev. Lett*. **2000**, *84*, 2961.
27. Chandrasekaran, K.; Vijayaraghaven, R.; Varadaraju, U. V. *Material Chem. & Phys*. **1998**, *56*, 63.
28. Demourgues, A.; Wattiaux, A.; Grenier, J. C.; Pouchard, M.; Soubeyroux, J. L.; Dance, J. M.; Hagenmueller, P. *J. Solid State Chem*. **1993**, *105*, 458.
29. Rial, C.; Moran, E.; Alario-Franco, M. A.; Amador, U.; Andersen, N. H. *Physica C* **1997**, *278*, 122.
30. Kamenev, K. V.; Lees, M. R.; Balakrishnan, G.; McK. Paul, D.; Marshall, W. G.; Tissen, V. G.; Nefedova, M. V. *Phys. Rev. Lett*. **2000**, *84*, 2710.
31. Moritomo, Y.; Hirota, K.; Nakao, H.; Kiyama, T.; Murakami, Y.; Okamoto, S.; Ishihara, S.; Maekawa, S.; Kubota, M.; Yoshizawa, H. *Phys. Rev. B* **2000**, *62*, 17.